Vision Research 48 (2008) 2284–2292

Contents lists available at ScienceDirect

Vision Research

journal homepage: www.elsevier.com/locate/visres

A mechanistic inter-species comparison of spatial contrast sensitivity

John R. Jarvis *, Christopher M. Wathes

The Royal Veterinary College, University of London, Hawkshead Lane, North Mymms, Hatfield, Herts AL9 7TA, UK

ARTICLE INFO

Article history:
Received 30 October 2007
Received in revised form 1 July 2008

Keywords:
Modulation transfer function
Spatial contrast sensitivity
Vertebrate
Acuity
Lateral inhibition
Optical attenuation

ABSTRACT

The validity of the Rovamo–Barten modulation transfer function model for describing spatial contrast sensitivity in vertebrates was examined using published data for the human, macaque, cat, goldfish, pigeon and rat. Under photopic conditions, the model adequately described overall contrast sensitivity for changes in both stimulus luminance and stimulus size for each member of this diverse range of species. From this examination, optical, retinal and post-retinal neural processes subserving contrast sensitivity were quantified. An important retinal process is lateral inhibition and values of its associated point spread function (PSF) were obtained for each species. Some auxiliary contrast sensitivity data obtained from the owl monkey were included for these calculations. Modeled values of the lateral inhibition PSF were found to correlate well with ganglion cell receptive field surround size measurements obtained directly from electrophysiology. The range of vertebrates studied was then further extended to include the squirrel monkey, tree shrew, rabbit, chicken and eagle. To a first approximation, modeled estimates of lateral inhibition PSF width were found to be inversely proportional to the square root of ganglion cell density. This finding is consistent with a receptive field surround diameter that changes in direct proportion to the distance between ganglion cells for central vision. For the main species examined, contrast sensitivity is considerably less than that for the human. Although this is due in part to a reduction in the performance of both optical and retinal mechanisms, the model indicates that poor cortical detection efficiency plays a significant role.

1. Introduction

Contrast sensitivity as determined from spatial sine-wave gratings, has now become a common indicator of the ability of the human visual system to process spatial frequency information (De Valois & De Valois, 1990; Regan, 1991). At a given grating spatial frequency, contrast sensitivity is defined as the inverse of Michelson contrast at the threshold of grating detection. As spatial frequency increases from low values, photopic contrast sensitivity typically increases, passes through a maximum and then decreases toward unity at a limiting frequency value often referred to as "acuity". Contrast sensitivity has also been directly measured for a diverse range of animals using both behavioural and electrophysiological techniques. From a study of published behavioural data, Uhlrich, Essock, and Lehmkuhle (1981) have illustrated that in virtually all animals, contrast sensitivity also displays a band-pass characteristic, although the magnitude of the contrast sensitivity function and associated frequency range vary considerably from species to species.

It is now generally accepted that three important pre-cortical processes contribute to spatial vision as characterized by contrast sensitivity in both the human and non-human species. The first is image formation through basic eye optics and the second is signal loss through the discrete spatial organization of retinal receptors. The third process is high-pass spatial filtering through lateral inhibition mediated by horizontal and amacrine cells. The combined effect of all these processes produces the band-pass characteristic of the contrast sensitivity function.

A theoretical model of these processes and how they link together has now been developed using the modulation transfer function (MTF) concept. Two versions of essentially the same model have been published by Barten (1999) and in a series of papers by Rovamo and co-workers (Rovamo, Kankaanpaa, & Kukkonen, 1999; Rovamo, Luntinen, & Nasanen, 1993; Rovamo, Mustonen, & Nasanen, 1994). The applicability of the Rovamo–Barten model for human vision has already been demonstrated by Barten (1999) using published data obtained for a range of stimulus and viewing conditions. These include changes in grating mean luminance (Patel, 1966; van Meeteren & Vos, 1972; van Nes & Bouman, 1967), grating size (Carlson, 1982; Rovamo et al., 1993), number of stimulus cycles (Virsu & Rovamo, 1979) and retinal eccentricity (Kelly, 1984: Robson & Graham, 1981; Virsu & Rovamo, 1979). It has also been shown that the Rovamo–Barten model can be used to derive the optical modulation transfer function from vertebrate contrast sensitivity data (Jarvis & Wathes, 2007).

* Corresponding author. Fax: +44 (0) 1707 666298.
E-mail address: jjarvis@rvc.ac.uk (J.R. Jarvis).

0042-6989/$ - see front matter © 2008 Elsevier Ltd. All rights reserved.
doi:10.1016/j.visres.2008.07.002

We will show in this communication that the Rovamo–Barten model can be used to describe overall spatial contrast sensitivity in a diverse range of species. By an analysis of the mathematical form of the model, we will also show that basic retinal and post-retinal mechanisms controlling contrast sensitivity can be quantified and directly compared on an inter-species basis. Where possible, these results are compared with mechanistic evaluations determined by electrophysiology. This work extends our previous study of vertebrate spatial vision (Jarvis & Wathes, 2007) and parallels the MTF-based modelling conducted on vertebrate temporal vision (Jarvis, Prescott, & Wathes, 2003; Jarvis, Taylor, Prescott, Meeks, & Wathes, 2002).

2. The model and its application

2.1. The Rovamo–Barten MTF model

The basic Rovamo–Barten model is summarized in Fig. 1. In this scheme, O represents the MTF associated with the combined effect of optics and retinal sampling, and H represents the MTF associated with lateral inhibition in the retina. The symbol u denotes spatial frequency (c.deg^{-1}). Photon noise (N_{qt}) is added at the point of quantal absorbtion by the photoreceptors and in the human visual system has a significant impact on contrast sensitivity at low luminances. Neural noise (N_{it}) is also included in the model. Spatial contrast sensitivity (S) is defined as,

$$S(u) = m(u)^{-1} \quad (1)$$

where m denotes the Michelson contrast of a sine-wave grating (of spatial frequency u c deg^{-1}) at the threshold of detection. The Rovamo–Barten model gives for S,

$$S(u) = K \cdot O(u) \cdot H(u) \cdot A(u) \cdot [N(u)]^{-0.5}, \quad (2)$$

where K and A relate to cortical signal detection and integration and define the final image interpretation stage of the model. The second term O in Eq. (2) is a product of both the MTF representing optical attenuation ($OMTF$) and the MTF representing the action of retinal sampling (MTF_r). The function N represents the total noise in the visual system and is a combination of photon and neural noise.

Each of the functions given in Eq. (2) are analytic and contain parameters which can be specifically related to both optical and neural mechanisms. In summary these parameters are u^* (which defines OMTF and represents the spatial frequency at half its maximum value), σ (which defines MTF_r and represents the standard deviation of the ganglion cell sampling line spread function), u_o (which defines H and represents the spatial frequency above which lateral inhibition ceases to operate), X_{max}, R_{max} (which define A and represent upper size and frequency limits respectively of spatial integration), N_{it} (which partially defines N and represents neural noise in the visual system), η (quantum efficiency) and K (cortical detection). Full mathematical descriptions of O, H, A, N and K together with the methods used to evaluate numerical values for their parameters are given in the Appendix. To facilitate the practical evaluation of these parameters, η and Nit are combined to define the new parameter (η N_{it}). This procedure leads to the quantification of a "system detection efficiency" term $\sqrt{\eta}\,K$. Theoretically, a given species will be defined by a unique set of parameter values which fully quantify the optical and neural mechanisms affecting its spatial contrast sensitivity.

2.2. Application of the model to measured spatial contrast sensitivity

2.2.1. Variation in stimulus size

The Rovamo–Barten model predicts an increase in low frequency contrast sensitivity as grating size increases (see Eq. (A12), Section A.4.2 of the Appendix). For a given species, this behaviour can be examined and the numerical parameter X_{max} contained within the model function A in Eq. (2) evaluated, providing contrast sensitivity measurements are available for two grating sizes. At least six individual species (including the human) can be identified where contrast sensitivity has been measured for this stimulus requirement. These are the macaque (measured for grating sizes of 2 deg (De Valois, Morgan, & Snodderley, 1974) and 6.8 deg (Smith, Harwerth, & Crawford, 1985), humans (measured for a range of grating sizes from 0.5 to 60 deg (Carlson,1982)), the pigeon (grating sizes of 8 and 30 deg (Hodos, Ghim, Potocki, Fields, & Storm, 2002)), the cat (grating sizes of 8 deg (Blake, Cool, & Crawford, 1974), 12 deg (Pasternak & Merigan, 1981) and 19 deg (Bisti & Maffei, 1974)), the hooded rat (grating sizes of 20 and 60 deg (Legg, 1984)), and the goldfish (grating sizes of 20 deg (Northmore & Dvorak, 1979) and 40 deg (Bilotta & Powers, 1991)). The data points in Fig. 2 are contrast sensitivity measurements obtained from these studies. The frequency axis in Fig. 2 (and also Figs. 3 and 4 in this communication) has been plotted as $u \times 10$ (c deg^{-1}) to assist in visual clarity. Measured contrast sensitivity for each species (except one data set for the cat), follows predictions given from the Rovamo–Barten model, ie a low frequency increase in contrast sensitivity as grating size increases. The curves in Fig. 2 represent these predictions, where for each species, parameter values were calculated according to the procedures outlined in the Appendix (Section A.4). As shown in the Appendix, to numerically define the complete set of parameters for a given species, measured contrast sensitivity data must also be available at two luminance levels. This data requirement has been met for the six species outlined above and details of these studies given in Section 2.2.2 below. The model parameter values calculated from these data are given in Tables 1 and 2.

All measured contrast sensitivity values given in Fig. 2 are from behavioural experiments except for the pigeon data for a grating size of 30 deg, which were obtained by Hodos et al., 2002 from the pattern electroretinogram (PERG). In the pigeon comparison, both the PERG and the behavioural 8 deg data are for an 8 Hz flicker presentation of the grating stimulus. Behavioural contrast sensitivity is higher than that obtained from the PERG by a factor which

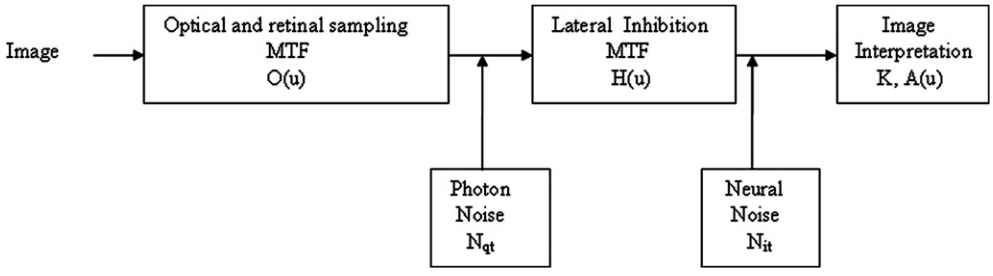

Fig. 1. Schematic representation of the Rovamo–Barten model for spatial contrast sensitivity. Symbols defined in the main text.

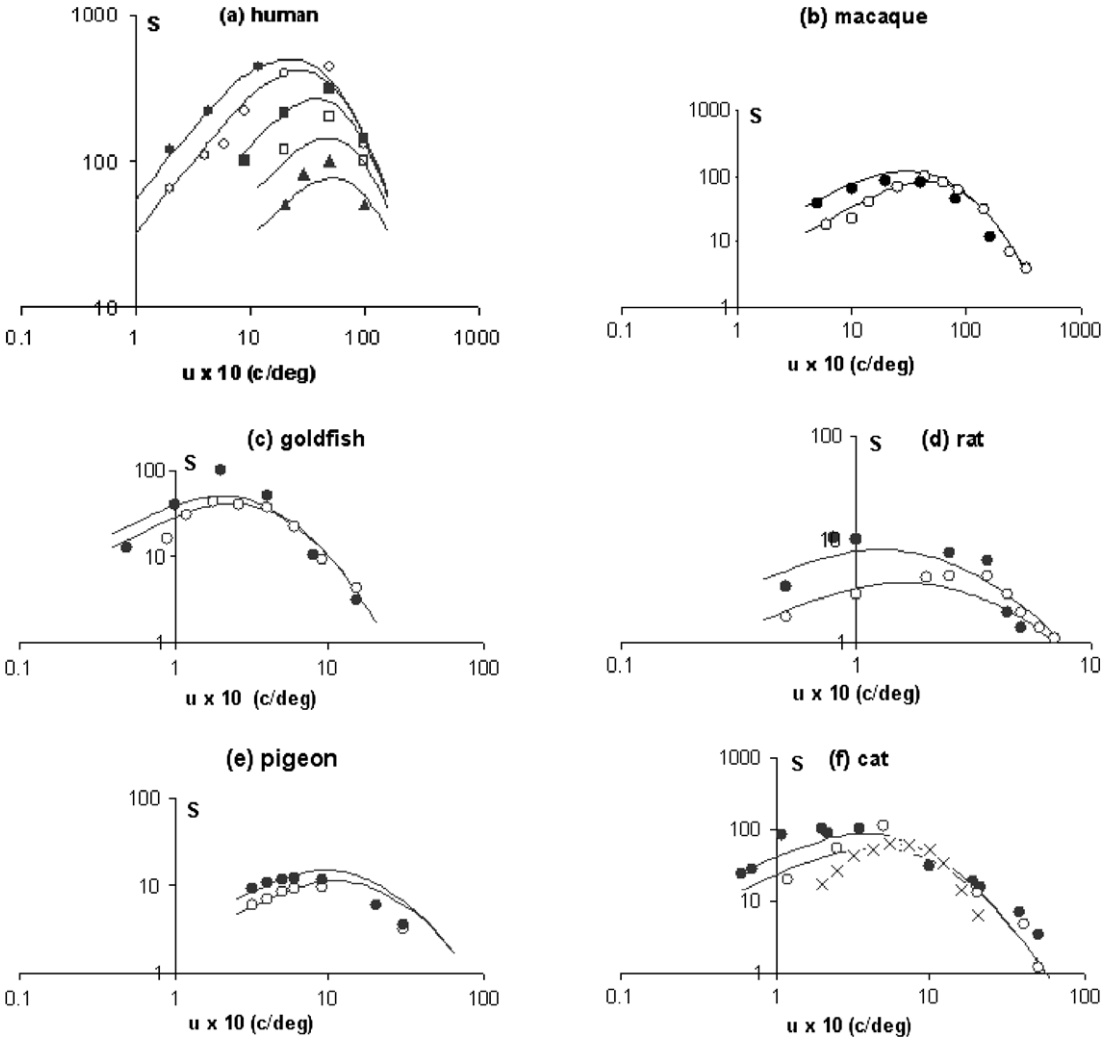

Fig. 2. Variation in spatial contrast sensitivity (S) with stimulus (grating) size. Data points are measured values, and curves represent the Rovamo–Barten model predictions. Model parameter values as defined in Table 1 (a) Human. Target sizes; 60 deg (filled circles), 6.5 deg (open circles), 2.3 deg (filled squares), 1.0 deg (open squares), 0.5 deg (filled triangles). (b) Macaque. Target sizes; 6.8 deg (filled circles), 2 deg (open circles). (c) Goldfish. Target sizes; 40 deg (filled circles), 20 deg (open circles). (d) Rat. Target sizes; 60 deg (filled circles), 20 deg (open circles). (e) Pigeon. Target sizes; 30 deg (filled circles), 8 deg (open circles). (f) Cat. Target sizes; 19 deg (filled circles), 8 deg (open circles), 12 deg (crosses).

is approximately constant at all frequencies (Hodos et al., 2002). The PERG data for the pigeon in Fig. 2 have therefore been increased by a factor of 2.8, this being the value which results in an overlay of the high frequency data for both experimental conditions. It will be noted that the high frequency measured data for the pigeon are lower than that predicted from the model. This is expected, because a flicker presentation of the stimulus significantly lowers high frequency contrast sensitivity in the pigeon. At low frequencies, 8Hz flicker has only a small effect on contrast sensitivity compared with steady state (0 Hz) presentation (Hodos, Potocki, Ghim, & Gaffney, 2003).

With reference to the cat results shown in Fig. 2, the Pasternak and Merigan (1981) data for a 12 deg grating are not consistent with the results obtained from the other two studies (Bisti & Maffei, 1974; Blake et al., 1974). The Pasternak & Merigan data (shown as crosses) indicate a higher degree of low-frequency loss in sensitivity.

2.2.2. Variation in stimulus luminance

The data points in Fig. 3 represent measured contrast sensitivity values for a range of grating mean luminance levels for the species examined in Sections 2.2.1. These data are from; van Meeteren and Vos (1972) (human observers), De Valois et al. (1974) (macaque), Bilotta and Powers (1991) (goldfish), Birch and Jacobs (1979) (rat), Ghim (1997) (pigeon) and Pasternak and Merigan (1981) (cat). The results shown in Fig. 3 have been re-expressed in terms of contrast sensitivity/mean luminance (S/L). This particular term, usually referred to as "amplitude sensitivity", gives a clearer representation of contrast sensitivity in graphs showing results for a wide range of stimulus luminances. Note that the ratio (S/L) increases as stimulus luminance decreases. The curves in Fig. 3 are modeled values of (S/L) with parameter values given in Tables 1 and 2. For each species, good agreement is seen between measured and modeled contrast sensitivity except at very low luminances. This deviation between measurement and theory is particularly pronounced for the cat. The model also gives a poor representation of low frequency sensitivity with this particular data.

In the model calculations given in Sections 2.2.1 and 2.2.2, the parameter ηN_{it} was determined for each species from contrast sensitivity measurements obtained at the highest and second highest luminance level (see Section A.4.4 of the Appendix). Parameter R_{max} was evaluated from contrast sensitivity at the highest luminance level (see Section A.4.6 for details) and the optical parameter u^* evaluated for each luminance from high frequency

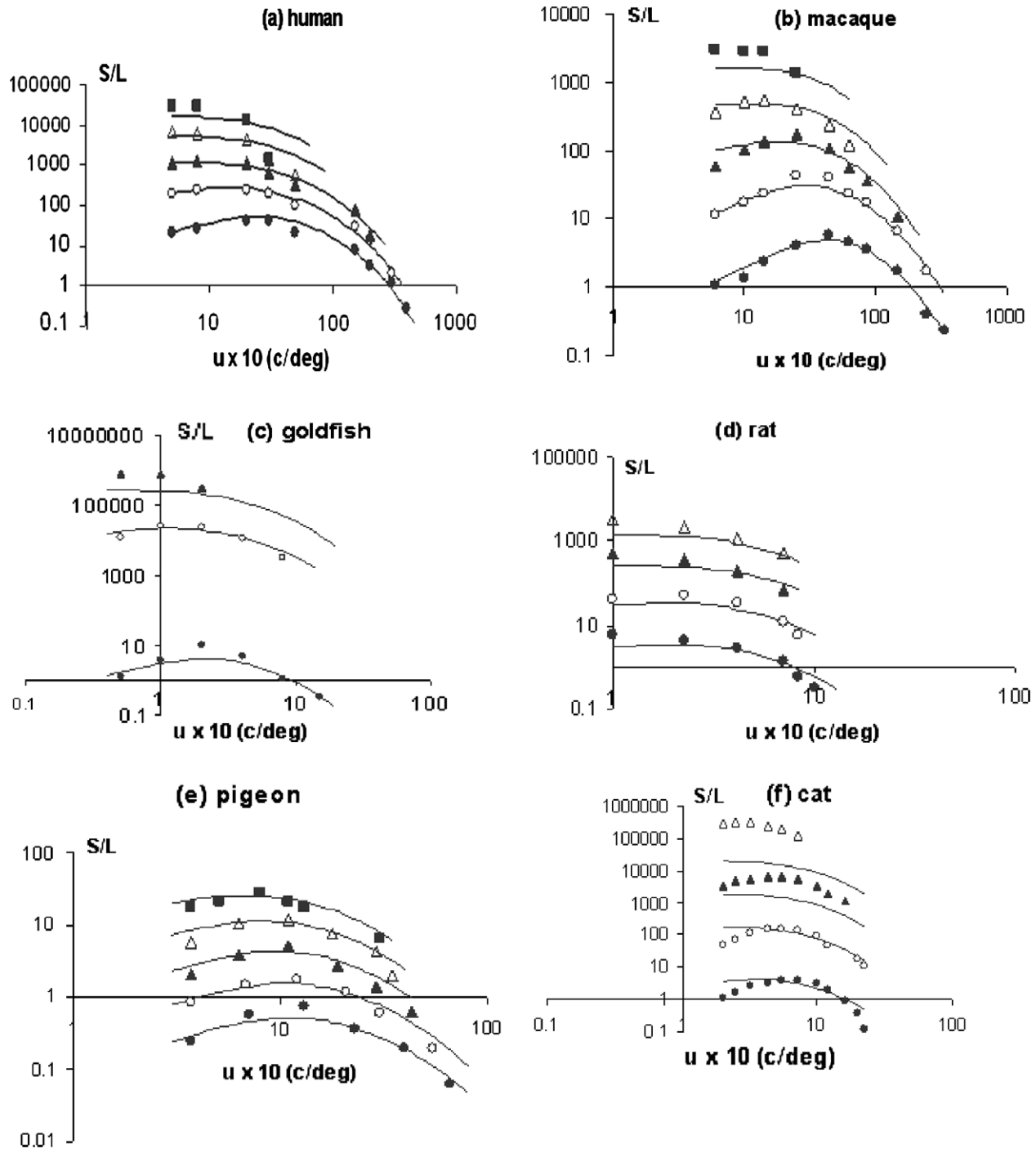

Fig. 3. Variation in spatial amplitude sensitivity (*S/L*) with stimulus luminance. *S* denotes contrast sensitivity and *L* denotes mean grating luminance. Data points are measured values, and curves represent the Rovamo–Barten model predictions. In each graph, *S/L* increases with decreasing luminance at any given frequency. Model parameter values are given for each species in Tables 1 and 2. (a) Human. Luminance levels; 10.0 (filled circles), 1.0 (open circles), 0.1 (filled triangles), 0.01 (open triangles) and 0.001 (filled squares) cd m^{-2}. (b) Macaque. Luminance levels; 17.1 (filled circles), 1.17 (open circles), 0.17 (filled triangles), 0.017 (open triangles) and 0.0017 (filled squares) cd m^{-2}. (c) Goldfish. Luminance levels; 10.0 (filled circles), 0.001 (open circles), 0.00001 (filled triangles) cd m^{-2}. (d) Rat. Luminance levels; 3.4 (filled circles), 0.34 (open circles), 0.034 (filled triangles), 0.0034 (open triangles) cd m^{-2}. (e) Pigeon. Luminance levels; 16.0 (filled circles), 5.0 (open circles), 1.6 (filled triangles), 0.5 (open triangles) and 0.16 (filled squares) cd m^{-2}. (f) Cat. Luminance levels; 16.0 (filled circles), 0.16 (open circles), 0.0016 (filled triangles), and 0.000016 (open triangles) cd m^{-2}.

data (see Section A.4.1) The sampling parameter σ for the human, goldfish, rat, pigeon and cat was obtained from Jarvis and Wathes (2007). For the macaque, σ was calculated in the manner given elsewhere (Jarvis & Wathes, 2007) using ganglion cell density data published by Pettigrew, Dreher, Hopkins, McCall, and Brown (1988). Retinal illuminance (*I*) values required in the model calculations (see Section A.1 in the Appendix) were determined from pupil size and PND data as described elsewhere (Hughes, 1977; Jarvis, et al., 2003). PND values for human observers, goldfish, rat, pigeon and cat were taken from Jarvis and Wathes (2007) and that for the macaque from Pettigrew et al. (1988). Pupil size data for the appropriate luminance level were obtained from Le

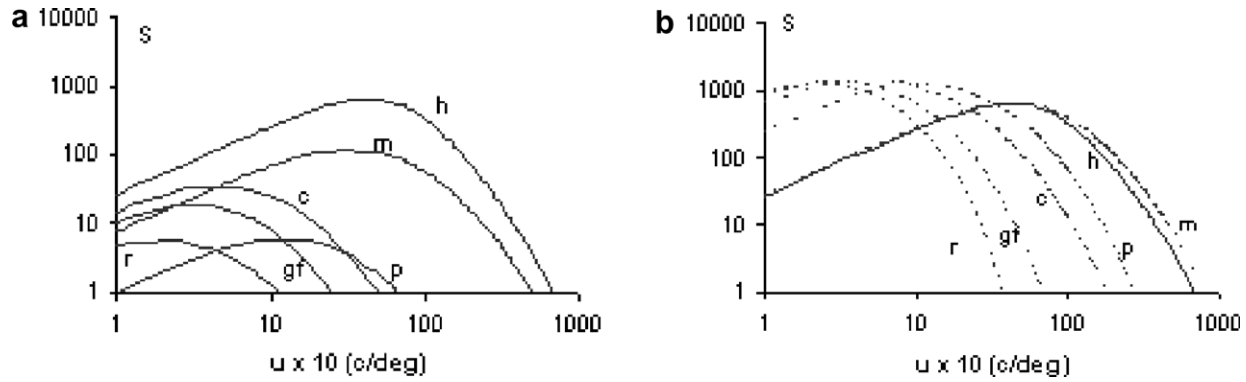

Fig. 4. (a) Theoretical contrast sensitivity (Rovamo–Barten) model for the human observer (h), macaque (m), cat (c), pigeon (p) goldfish (gf) and rat (r). Comparison is for a fixed retinal illuminance of 1000 Td and grating size of 5 deg. (b) As for Fig. 4 a, but with each species having the human system detection efficiency ($\sqrt{\eta}\cdot K$) and noise ($\eta \cdot N_{it}$).

Table 1
Numerical values of the Rovamo–Barten model parameters for six species including the human observer

	$\sqrt{\eta}\,K\,s^{0.5}$	u_o c deg^{-1}	X_{max} deg	R_{max} cycles	σ arc min	$\eta\,N_{it}$ s deg^2
Human	1.28×10^{-2}	7.0	9.0	30.1	0.15	9.0×10^{-10}
Macaque	2.7×10^{-3}	7.0	8.0	9.0	0.15	9.0×10^{-10}
Goldfish	1.9×10^{-3}	0.2	23.0	4.0	2.4	3.1×10^{-7}
Rat	9.7×10^{-5}	0.1	81.0	10.2	6.29	1.8×10^{-7}
Pigeon	1.14×10^{-4}	0.8	9.8	12.2	0.665	4.2×10^{-9}
Cat	4.0×10^{-4}	0.3	16.7	7.48	0.93	1.8×10^{-9}

$\sqrt{\eta}\cdot K$ = system detection efficiency (where η denotes quantum efficiency and K cortical detection factor).
u_o = spatial frequency above which lateral inhibition ceases.
X_{max} = upper size limit for spatial integration.
R_{max} = upper frequency limit for spatial integration.
σ = standard deviation of the ganglion cell sampling line spread function.
$\eta \cdot N_{it}$ = system noise term.

Table 2
Numerical values of the optical parameter u^* for six species including the human observer

	u^*_1 c deg^{-1}	u^*_2 c deg^{-1}	u^*_3 c deg^{-1}	u^*_4 c deg^{-1}	u^*_5 c deg^{-1}
Human	9.0	8.0	6.5	5.1	4.4
Macaque	16.0	14.0	10.0	8.4	7.1
Goldfish	1.15	1.15	1.15	—	—
Rat	0.63	0.6	0.58	0.58	—
Pigeon	5.91	4.9	3.9	3.4	3.0
Cat	1.6	1.29	1.29	1.29	—

Subscript number scale 1–5 denotes increasing levels of stimulus luminance. For a given species, luminance levels are as indicated in Fig. 3.

Grand (1968) (human), Clarke, Zhang, and Gamlin (2003) (macaque), Jarvis and Wathes (2007) (goldfish), Hughes (1977) (rat), Ghim (1997) (pigeon) and Hammond and Mouat (1985) (cat).

2.3. Theoretical inter-species comparison

Determination of the numerical value of individual parameters in the Rovamo–Barten model enables a detailed study to be made of inter-species differences in contrast sensitivity. The first inter-species performance comparison is shown in Fig. 4a which illustrates modeled contrast sensitivity curves at a fixed retinal illuminance of 1000 Td and grating size of 5 deg. This particular comparison shows the theoretical performance differences between species for a photometrically balanced light level input to the visual neural system. For each species, u^* was estimated from the variation found in this optical parameter as a function of luminance when the modeled curves in Fig. 3 were derived. All other parameters are as given in Table 1. In this particular comparison, overall performance (as reflected by maximum sensitivity) is ranked; human observers, macaque, cat, goldfish, pigeon and rat. The theoretical curves clearly show the superior overall contrast sensitivity performance of the human observer compared with all other species. The parameter values of Tables 1 and 2 also show that all species (except the macaque) display both a reduced optical performance and retinal sampling capacity compared with the human visual system. These particular reductions in visual performance account for much of the high frequency sensitivity loss observed in the cat, goldfish, pigeon and rat. A key question, however, is how do other neural factors individually influence overall contrast sensitivity.

To answer this basic question, trial parameter variations in the model were carried out. These revealed that a reduction in value of the cortical information summation factors X_{max} and R_{max} in the model will decrease contrast sensitivity at low and high spatial frequency respectively. The variation in sensitivity associated with a change in both parameters is, however, relatively small for the range of values shown in Table 1. A decrease in the lateral inhibition parameter u_o increases low frequency response and therefore cannot account for any of the sensitivity losses shown by individual species compared with the human observer. The most important factors affecting the overall magnitude of the contrast sensitivity function (particularly the maximum value) are overall system detection efficiency and system noise as quantified by the two parameter products $\sqrt{\eta}\,K$ and $\eta\,N_{it.}$ The importance of these factors in controlling overall contrast sensitivity is illustrated in Fig. 4b. The inter-species comparison is again for a retinal illuminance of 1000 Td, but now each species has the system detection efficiency ($\sqrt{\eta}\,K$) and noise factor ($\eta\,N_{it}$) values for the human system. The contrast sensitivity curves for the cat, goldfish, pigeon and rat all now display similar peak sensitivity. The fact that the curves for these species

are slightly higher than for the human observer (and macaque) at low frequencies can be accounted for by the reduced value of the lateral inhibition parameter u_o.

3. Physiological correlations

As outlined above, three important pre-cortical processes contribute to vertebrate spatial vision, namely optical attenuation, retinal sampling and lateral inhibition. An analysis of both retinal sampling and optical attenuation factors in a range of vertebrates, verified that the Rovamo–Barten model provides a realistic mechanistic description of both processes (Jarvis & Wathes, 2007). This section addresses the lateral inhibition component of the model as quantified by the parameter u_o and examines its relationship with known retinal physiology.

The MTF for lateral inhibition (H) in the model (Eq. (2)) describes the action of a high pass filter. The mechanism involved is, however, one where a low pass filtered signal is subtracted from a signal derived directly from the photoreceptors ie.

$$H(u) = 1 - F(u) \tag{3}$$

where F is the MTF of the spatial low pass filter. As shown in the Appendix (Section A.2), the function H is given by,

$$H(u) = [1 - exp(-(u/u_o)^2)] \tag{4}$$

where the parameter u_o represents the spatial frequency above which the action of lateral inhibition ceases.

Combining Eqs. (3) and (4) gives;

$$F(u) = 1 - [1 - \exp(-(u/u_o)^2)]^{0.5} \tag{5}$$

The point spread function (PSF) associated with Eq. (5) gives a radial distance measure of the inhibiting surround signal. The PSF is provided by the Hankel transform of Eq. (5), but unfortunately no analytic expression exists for the mathematical form of this equation. Barten (1999) has, however, shown that Eq. (5) can be closely approximated by the expression,

$$F(u) = 0.5 \cdot [\exp(-2(u/u_o)) + \exp(-(u/u_o)^2)] \tag{6}$$

An analytic expression exists for the Hankel transform of Eq. (6) and is given by,

$$f(r) = 0.25 \cdot \pi \cdot u_o^2 \cdot (1 + \pi^2 u_o^2 r^2)^{-1.5} + 0.5 \cdot \pi \cdot u_o^2 \cdot \exp(-\pi^2 u_o^2 r^2) \tag{7}$$

where r denotes radial distance. Eq. (7) represents the receptive field of the inhibition process where the parameter u_o is inversely proportional to its radius (Barten, 1999).

It is now well accepted that the antagonistic surround region of the ganglion cell receptive field represents a basic "point mechanism" for lateral inhibition in the retina. This mechanism appears in most vertebrate and invertebrate species (Land, 1985). Within a single retina, many studies have shown that ganglion cell receptive fields vary in both size and the spatial frequency tuning resulting from lateral inhibition (eg. Bernadete & Kaplan, 1997; Croner & Kaplan, 1995; Enroth-Cugell & Robson, 1966; Enroth-Cugell, Robson, Schweitzer-Tong, & Watson, 1983; Xu, Bonds, & Casagrande, 2002). Ganglion cells also differ in the type of information they output. In the primate retina, some cells (P-cells) project through to the parvocellular target in the lateral geniculate nucleus (LGN). Others project through to the magnocellular and koniocellular target regions; M-cells, and K-cells respectively. Therefore specifying a physiological correlate of the lateral inhibition receptive field described by Eq. (7) offers difficulties. It would seem probable, however, that this equation quantifies some mean or average ganglion cell receptive field surround size. The approach now taken to elucidate the physiological substrate of Eq. (7) is to compare model calculations of receptive field size with size data obtained through electrophysiology.

The first comparison is for the cat, where ganglion (and LGN) cell receptive field profiles have been directly mapped (Kaplan, Marcus, & So, 1979). The data points in Fig. 5 are measurements of the antagonistic surround field profile for both a cat X-on centre ganglion cell and Y-on centre LGN cell. Cells identified as X and Y in the cat are considered equivalent to P- and M-cells respectively. The X-cell receptive field profiled by Kaplan et. al. has a size very close to the mean value found in a study of 21 ganglion X-cells in the cat retina (Enroth-Cugell & Robson, 1966). The curve in Fig. 5 represents f (Eq. (7)) with the parameter u_o placed equal to 0.3 c deg $^{-1}$, this being the value found for the cat. Note that $-f$ is plotted to illustrate the antagonistic or negative-working behaviour of the surround field. Values of $-f$ have also been normalised to fit the data near $r = 0$. A good fit is seen between Eq. (7) and the directly measured data.

Electrophysiology has also revealed ganglion cell receptive field dimensions in a number of other species and these include the macaque, owl monkey, goldfish and rat. Fig. 6 shows directly measured estimates of ganglion cell receptive field surround radius (r_s) for these species plotted against u_o^{-1}. The value of u_o for the owl monkey was calculated from low frequency contrast sensitivity data measured by Jacobs (1977) and the remainder as specified in previous sections. Values of r_s in Fig. 6 are given for P-cells (solid circles), M-cells (open circles) and non-specified (triangles). Each value of r_s represents a mean value for ganglion cells contained within the central viewing region. Measured size data were obtained from Lee, Kremers, and Yeh (1998) and Croner and Kaplan (1995) for the macaque, (Xu et al., 2002) for the owl monkey, Kaplan et al. (1979) and Enroth-Cugell and Robson (1966) for the cat, Partridge and Brown (1970) for the rat, and Daw (1968) for the goldfish. The value of r_s for the human visual system was not derived from electrophysiology, but from the psychophysical study performed by Blommaert, Heijnen, and Roufs (1987). These authors directly estimated the human PSF associated with lateral inhibition through detection thresholds for a small spot light stimulus contained within an annular surround. The general trend for the data of Fig. 6 conforms to the theoretical prediction that r_s is inversely proportional to u_o.

Finally, Fig. 7 shows log (u_o) plotted against log (G) where G denotes maximum ganglion cell density. Data for the eagle, rabbit, tree shrew, squirrel monkey and chicken are added in this examination. The extra calculations of u_o were carried out from published behavioural contrast sensitivity from Reymond and Wolfe (1981) for the eagle, Merigan (1976) for the squirrel monkey,

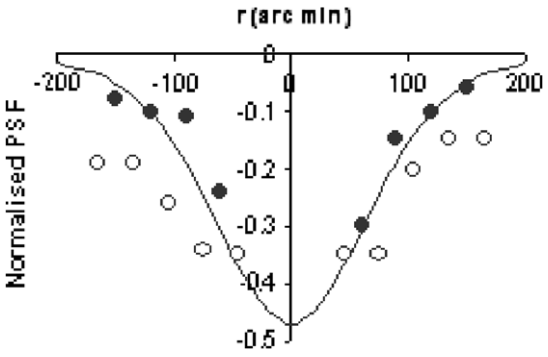

Fig. 5. Measurements of the receptive field surround profile for a cat X-on ganglion cell receptive field surround (filled circles) and Y-on LGN cell receptive field surround (open circles). The curve is the modeled point spread function for retinal lateral inhibition in the cat.

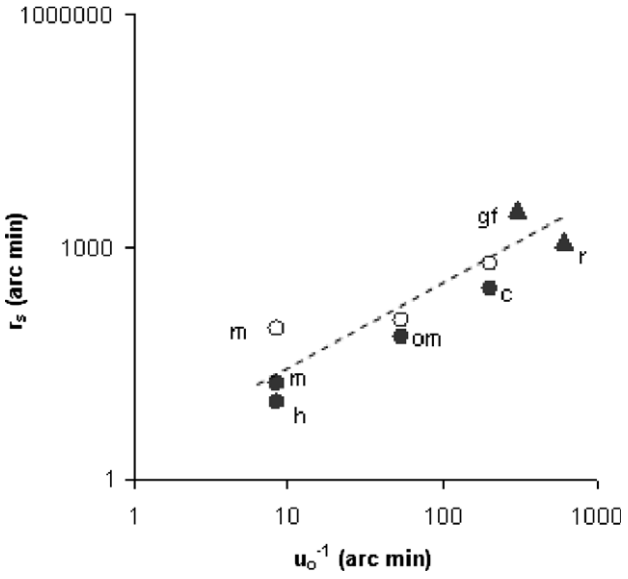

Fig. 6. Directly measured ganglion cell receptive field surround radius r_s plotted against parameter u_o^{-1}. P-Cells (filled circles), M-cells (open circles), unspecified (filled triangles). Species classification as in Fig. 4, with the addition of owl monkey (om).

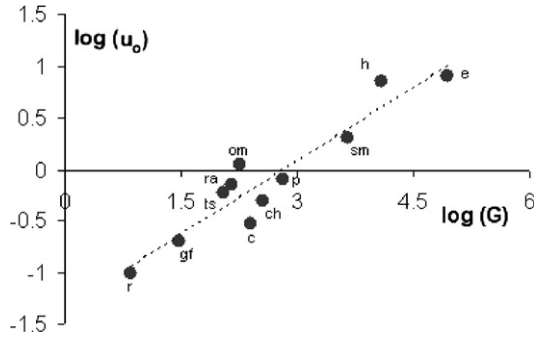

Fig. 7. Relationship between parameter u_o and ganglion cell density G. The slope of the linear regression line is 0.47. Species classification as in Figs. 4 and 6 with the addition of eagle (e), squirrel monkey (sm), chicken (ch), rabbit (ra) and tree shrew (ts).

Petry, Fox, and Casagrande (1984) for the tree shrew, Abeyesinghe, McMahon, Jarvis and Wathes (2007) for the chicken, and visually evoked cortical responses (VECPs) obtained by Pak (1984) for the rabbit. Ganglion cell density figures were obtained from Jarvis and Wathes (2007) for the owl monkey, tree shrew, and chicken, from Rolls and Cowey (1970) for the squirrel monkey, and from Pettigrew et al. (1988) for the eagle and rabbit. The interesting feature of Fig. 7 is that the slope of the linear regression line shown is almost exactly 0.5. This finding is consistent with a ganglion cell receptive field surround radius that changes in direct proportion to the distance between ganglion cells with central vision.

4. Discussion

Vertebrate spatial contrast sensitivity can be represented by the Rovamo–Barten model for most of the species and stimulus conditions examined. A feature of this model is that all of the intrinsic mathematical parameters can be readily related to a specific optical or neural mechanism in the visual system. Once the set of parameter values have been calculated for a given species, the model is seen to be extremely robust in its predictive power when applied to data obtained under a wide range of experimental and laboratory conditions. An inspection of the results shown in Fig. 3, however, reveals a slight underestimation of low frequency contrast sensitivity for the lowest luminance levels in humans, the macaque and the goldfish. This limitation of the model has been found before in the study of human spatial contrast sensitivity conducted by Barten (1999). The design of the model is fundamentally for photopic viewing conditions, and so the failure indicated at low light levels has been attributed by Barten to a switch from cone to rod vision. Certainly the two lowest light levels shown in Fig. 3a are scotopic for the human system (Schlaer, 1937), and the lowest in Fig. 3 c is scotopic for the goldfish (Bilotta & Powers, 1991). On the other hand, Rovamo et al., 1994 do not find this limitation when the model is applied to their own scotopic measurements.

The one data set where only approximate correlations are achieved between theory and measurement is that from Pasternak and Merigan (1981). As shown in Fig. 3f, the modeled curves deviate significantly from the low frequency data given in their study. This is because the model parameters (except for η N_{it}) have values based on an analysis of contrast sensitivity measured by both Blake et al. (1974) and Bisti and Maffei (1974). As shown in Fig. 2f, the Pasternak & Merigan result indicates significantly less low frequency sensitivity in the cat compared with the other two studies. The reasons for the disparity between the Pasternak & Merigan study and the other two are unclear. Again, considerable variation between model and measurement at all frequencies is seen for the two lowest luminance conditions in the Pasternak & Merigan data of Fig. 3f. These two luminance levels are well below the scotopic transition point for the cat and so the breakdown of the model may simply be due to the switch to rod vision.

In general, a reduction in stimulus luminance also leads to a more low-pass characteristic for the contrast sensitivity function. The Rovamo–Barten model predicts this behaviour, which is a consequence of high photon noise. For this condition, total internal noise N tends toward H^2 N_{qt} (see Eq. (A1) in the Appendix). The lateral inhibition term H (which controls the band-pass behaviour of the contrast sensitivity function) then cancels out in the main model expression (Eq. (2)). This loss in lateral inhibition is consistent with recent theoretical studies of the role played by the retina in improving signal/noise ratio at low luminances (Graham, Chandler, & Field, 2006). Electrophysiological data of ganglion cell receptive field characteristics also reveal a reduction or complete loss of lateral inhibition at low luminances in the cat (Kaplan et al., 1979; Peichl & Wassle, 1979). The physiological mechanism for this is, however, not fully understood. It is observed in these studies, that the measured receptive field centre expands considerably at low luminances. This could be due either to a reduction in the strength of the inhibitory surround or a masking of the surround by the enlargement of the receptive field centre. Such an expansion would take place to increase the photon catch from a basically low level input, with a consequential masking of the lateral inhibition mechanism.

For central vision, the receptive field size of the lateral inhibition process is modeled through the single parameter u_o and, as shown in Section 3, correlates reasonably well with directly measured (generic) ganglion field size data for a range of species. To some extent this analysis is facilitated because although ganglion cell receptive fields have a significant size distribution within a given species, there is a very large variation of the representative or mean size from species to species as shown in Fig. 6. There are, however, a number of issues relating to which type or types of ganglion cell are associated with u_o. For example, ganglion cells of the M-type and P-type convey luminance and colour information respectively and as a consequence of this functional difference, M-type have been suggested as cells subserving the spatial contrast sensitivity function (Barten, 1999; Plainis & Murray, 2005). This would link u_o with M-type ganglion cells. However, the

situation appears more complex, with the colour-responding P-cells conveying luminance information at high spatial frequencies, and M-cells luminance information at low frequencies (Lennie, 1993; Leonova, Pokorny, & Smith, 2003). For M-cells, this situation is reflected in a more low-pass MTF characteristic compared with P-cells. Xu et al. (2002). Psychophysical studies using narrow-band spatially-pulsed stimuli (Leonova et al., 2003) or chemically induced pathway lesions studies (Merigan & Maunsell, 1993) have also shown the overall M-pathway to be low-pass in character. The strong band-pass nature of the behavioural photopic contrast sensitivity function is reflected more by the shape of the P-pathway MTF. This raises the possibility that u_o may be associated with P-type ganglion cells. The good fit between the X-cell receptive field surround directly mapped by Kaplan et al. (1979) and the modeled profile shown in Fig. 5 would support this postulate. The increased importance of P-cells in central spatial vision is certainly consistent with the fact that their density is considerably higher than M-cells in many species. In the fovea, P/M cell ratio is about 0.95 in the human visual system (Dacey, 1993), and around 0.8 in both the cat (Peichl & Wassle, 1979) and the marmoset (Gomes, Silveira, Saito, & Yamada, 2005). However, any conclusions drawn from the limited data of Figs. 5–7 regarding the type of ganglion cell associated with u_o must be regarded as speculative.

Finally, it is of interest to discuss overall contrast sensitivity performance on a mechanistic inter-species basis. As Fig. 4 shows, all species examined have reduced overall contrast sensitivity compared with the human observer. For a given non-human species (excluding the macaque), the estimated signal transfer properties of all major stages in the visual process are inferior to the human (see Tables 1 and 2). As revealed in Section 2.3, poor optical performance and retinal sampling can account for the high frequency reduction in sensitivity in the cat, goldfish, pigeon and rat. The reduction in overall magnitude of the contrast sensitivity function in non-human species is, however, due mainly to reduced system detection efficiency (as quantified by $\sqrt{\eta K}$) and poor noise in the visual system (as reflected in a high value of ηN_{it}). The macaque offers an interesting comparison because model parameter estimations for this species reveal optical, receptor sampling, lateral inhibition and internal noise performance levels comparable to the human observer. Its maximum contrast sensitivity is, however, only around 20% that for humans (see Fig. 4a). If is assumed that the quantum efficiency (η) of this species is similar to that of the human system, then the reduction in overall contrast sensitivity displayed by the macaque stems entirely from a reduced cortical detection ability. The reduced overall contrast sensitivity of the cat may also be simply due to reduced cortical detection, since its quantum efficiency appears to be greater than for the human visual system (Bonds & MacCleod, 1974).

Acknowledgment

This research was funded by the BBSRC.

Appendix A. Supplementary data

Supplementary data associated with this article can be found, in the online version, at doi:10.1016/j.visres.2008.07.002.

References

Abeyesinghe, S. M., McMahon, C. E., Jarvis, J. R., & Wathes, C. M. (2007). *Behavioural determination of the hen's spatial contrast sensitivity. ISAE 41st Congress. Applying ethology to animal and ecosystem management*. Mexico: Merida. 30th July–3rd August.

Barten, P. J. G. (1999). *Contrast sensitivity of the human eye and its effects on image quality*. Washington: SPIE Optical Engineering Press.

Bernadete, E. A., & Kaplan, E. (1997). The receptive field of the primate P retinal ganglion cell. *I: linear dynamics. Visual Neuroscience, 14*, 169–186.

Bilotta, J., & Powers, M. K. (1991). Spatial contrast sensitivity of goldfish: Mean luminance, temporal frequency and a new psychophysical technique. *Vision Research, 31*, 577–585.

Birch, D., & Jacobs, G. H. (1979). Spatial contrast sensitivity in albino and pigmented rats. *Vision Research, 19*, 933–937.

Bisti, S., & Maffei, L. (1974). Behavioural contrast sensitivity of the cat in various visual meridians. *Journal of Physiology, 241*, 201–210.

Blake, R., Cool, S. J., & Crawford, M. L. J. (1974). Visual resolution in the cat. *Vision Research, 14*, 1211–1217.

Blommaert, F. J. J., Heijnen, H. G. M., & Roufs, J. A. J. (1987). Point spread functions and detail detection. *Spatial Vision, 2*, 99–115.

Bonds, A. B., & MacCleod, D. I. A. (1974). The bleaching and regeneration of rhodopsin in the cat. *Journal of Physiology, 242*, 237–253.

Carlson, C. R. (1982). Sine-wave threshold contrast-sensitivity function: Dependence on display size. *RCA Review, 43*, 675–683.

Clarke, R. J., Zhang, H., & Gamlin, P. D. R. (2003). Characteristics of the pupillary light reflex in the alert rhesus monkey. *Journal of Neurophysiology, 89*, 3179–3189.

Croner, L. J., & Kaplan, E. (1995). Receptive fields of P and M ganglion cells across the primate retina. *Vision Research, 35*, 7–24.

Dacey, D. M. (1993). The mosaic of midget ganglion cells in the human retina. *The Journal of Neuroscience, 13*, 5334–5355.

Daw, N. W. (1968). Colour-coded ganglion cells in the goldfish retina: Extension of their receptive fields by means of new stimuli. *Journal of Physiology, 197*, 567–592.

De Valois, R. L., Morgan, H., & Snodderley, D. M. (1974). Psychophysical studies of monkey vision—III. Spatial luminance contrast sensitivity tests of macaque and human observers. *Vision Research, 14*, 75–81.

De Valois, R. L., & De Valois, R. L. (1990). *Spatial vision. Oxford psychology series 14*. New York: Oxford University Press.

Enroth-Cugell, C., & Robson, J. G. (1966). The contrast sensitivity of retinal ganglion cells of the cat. *Journal of Physiology, 197*, 517–552.

Enroth-Cugell, C., Robson, J. G., Schweitzer-Tong, D. E., & Watson, A. B. (1983). Spatio-temporal interactions in cat retinal ganglion cells showing linear spatial summation. *Journal of Physiology, 341*, 279–307.

Ghim, M. M. (1997). *The effects of retinal illumination and target luminance on the contrast sensitivity function of pigeons Masters Thesis*. College Park: University of Maryland.

Gomes, F. L., Silveira, L. C. L., Saito, C. A., & Yamada, E. S. (2005). Density, proportion and dendritic coverage of retinal ganglion cells of the common marmoset (*Callithrix jacchus jacchus*). *Brazilian Journal of Medical and Biological Research, 38*, 915–924.

Graham, D. J., Chandler, D. M., & Field, D. J. (2006). Can the theory of "whitening" explain the centre-surround properties of retinal ganglion cell receptive fields? *Vision Research, 46*, 2901–2913.

Hammond, P., & Mouat, G. S. V. (1985). The relationship between feline pupil size and luminance. *Experimental Brain Research, 59*, 485–490.

Hodos, W., Ghim, M. M., Potocki, A., Fields, J. N., & Storm, T. (2002). Contrast sensitivity in pigeons: A comparison of behavioural and pattern ERG methods. *Documenta Ophthalmologica, 104*, 107–118.

Hodos, W., Potocki, A., Ghim, M. M., & Gaffney, M. (2003). Temporal modulation of spatial contrast vision in pigeons (*Columba livia*). *Vision Research, 43*, 761–767.

Hughes, A. (1977). The topography of vision in mammals of contrasting life style: Comparative optics and retinal organization. In F. Crescitelli (Ed.), *The visual system in vertebrates* (pp. 613–756). New York-Verlag: Springer.

Jacobs, G. H. (1977). Visual capabilities of the owl monkey (*aotus trivirgatus*). *Vision Research, 17*, 821–825.

Jarvis, J. R., Taylor, N. R., Prescott, N. B., Meeks, I., & Wathes, C. M. (2002). Measuring and modelling the photopic flicker sensitivity of the chicken (Gallus g domesticus). *Vision Research, 42*, 99–106.

Jarvis, J. R., Prescott, N. B., & Wathes, C. M. (2003). A mechanistic inter-species comparison of flicker sensitivity. *Vision Research, 43*, 1723–1734.

Jarvis, J. R., & Wathes, C. M. (2007). On the calculation of optical performance factors from vertebrate spatial contrast sensitivity. *Vision Research, 47*, 2259–2271.

Kaplan, E., Marcus, S., & So, Y. T. (1979). Effects of dark adaptation on spatial and temporal properties of receptive fields in cat lateral geniculate nucleus. *Journal of Physiology, 294*, 561–580.

Kelly, D. H. (1984). Retinal inhomogeneity I. Spatiotemporal contrast sensitivity. *Journal of the Optical Society of America, A, 1*, 107–113.

Land, M. (1985). The eye: optics. In G. A. Kerku & L. I. Gilbert (Eds.). *Comprehensive insect physiology, biochemistry and pharmacology*. London: Pergamon.

Lee, B. B., Kremers, J., & Yeh, T. (1998). Receptive fields of primate retinal ganglion cells studied with a novel technique. *Visual Neuroscience, 15*, 161–175.

Legg, C. R. (1984). Contrast sensitivity at low spatial frequencies in the hooded rat. *Vision Research, 24*, 159–161.

Le Grand, Y. (1968). *Light, colour and vision*. London: Chapman & hall.

Leonova, A., Pokorny, J., & Smith, V. C. (2003). Spatial frequency processing in inferred PC- and MC-pathways. *Vision Research, 43*, 2133–2139.

Lennie, P. (1993). Roles of M and P pathways. In R. Shapley & D. M. K. Lam (Eds.), *Contrast sensitivity*. Cambridge, MA: MIT Press.

Merigan, W. H. (1976). The contrast sensitivity of the squirrel monkey (Saimiri Sciureus). *Vision Research, 16*, 375–379.

Merigan, W. H., & Maunsell, J. H. R. (1993). How parallel are the primate visual pathways? *Annu. Rev. Neurosci, 16*, 369–402.

Northmore, D. P. M., & Dvorak, C. A. (1979). Contrast sensitivity and acuity of the goldfish. *Vision Research, 19*, 255–261.
Pak, M. A. (1984). Ocular refraction and visual contrast sensitivity of the rabbit, determined by the VECP. *Vision Research, 24*, 341–345.
Partridge, L. D., & Brown, J. E. (1970). Receptive fields of rat ganglion cells. *Vision Research, 10*, 450–455.
Pasternak, T., & Merigan, W. H. (1981). The luminance dependence of spatial vision in the cat. *Vision Research, 21*, 1333–1339.
Patel, A. S. (1966). Spatial resolution by the human visual system: The effect of mean retinal illuminance. *Journal of the Optical Society of America, 56*, 689–694.
Peichl, L., & Wassle, H. (1979). Size, scatter and coverage of ganglion cell receptive field centres in the cat retina. *J.Physiol, 291*, 117–141.
Petry, H. M., Fox, R., & Casagrande, V. A. (1984). Spatial contrast sensitivity of the tree shrew. *Vision Research, 24*, 1037–1042.
Pettigrew, J. D., Dreher, B., Hopkins, C. S., McCall, M. J., & Brown, M. (1988). Peak density and distribution of ganglion cells in the retinae of microchiropteran bats: Implications for visual acuity. *Brain Behaviour and Evolution, 32*, 39–56.
Plainis, S., & Murray, I. J. (2005). Magnocellular channel subserves the human contrast-sensitivity function. *Perception, 34*, 933–940.
Regan, D. (1991). Spatial vision. In J. Cronly-Dillon (Ed.), *Vision and visual dysfunction 10*. CRC: Boston.
Reymond, L., & Wolfe, J. (1981). Behavioural determination of the contrast sensitivity function of the eagle (Aquila Audax). *Vision Research, 21*, 263–271.
Robson, J. G., & Graham, N. (1981). Probability summation and regional variation in contrast sensitivity across the visual field. *Vision Research, 21*, 409–418.
Rolls, E. T., & Cowey, A. (1970). Topography of the retina and striate cortex and its relationship to visual acuity in rhesus monkeys and squirrel monkeys. *Experimental Brain Research*, 298–310.
Rovamo, J., Luntinen, O., & Nasanen, R. (1993). Modelling the dependence of contrast sensitivity on grating area and spatial frequency. *Vision Research, 33*, 2773–2788.
Rovamo, J., Mustonen, J., & Nasanen, R. (1994). Modelling contrast sensitivity as a function of retinal illuminance and grating area. *Vision Research, 34*, 1301–1314.
Rovamo, J., Kankaanpaa, M. I., & Kukkonen, H. (1999). Modelling spatial contrast sensitivity functions for chromatic and luminance-modulated gratings. *Vision Research, 39*, 2387–2398.
Schlaer, S. (1937). The relation between visual acuity and illumination. *Journal of General Physiology, 21*, 165–188.
Smith, E. L., Harwerth, R. S., & Crawford, M. L. J. (1985). Spatial contrast sensitivity deficits in monkeys produced by optically induced anisometropia. *Investigative Ophthalmology and Visual Science, 26*, 330–342.
Uhlrich, D. J., Essock, E. A., & Lehmkuhle, S. (1981). Cross-species correspondence of spatial contrast sensitivity functions. *Behavioural Brain Research, 2*, 291–299.
van Meeteren, A., & Vos, J. J. (1972). Resolution and contrast sensitivity at low luminance levels. *Vision Research, 12*, 825–833.
van Nes, F. L., & Bouman, M. A. (1967). Spatial modulation transfer in the human eye. *Journal of the Optical Society of America, 57*, 401–406.
Virsu, V., & Rovamo, J. (1979). Visual resolution, contrast sensitivity, and the cortical magnification. *Experimental Brain Research, 37*, 475–494.
Xu, X., Bonds, A. B., & Casagrande, V. A. (2002). Modeling receptive-field structure of koniocellular, magnocellular and parvocellular LGN cells in the owl monkey (*Aotus trivigatus*). *Visual Neuroscience, 19*, 703–711.